This manuscript is a non-peer-reviewed preprint submitted to EarthArXiv service. It can be cited as a preprint. The manuscript was submitted for consideration to the Planetary and Space Science journal on 3 February 2026. For any inquiries, feel free to visit https://terramakers.com for more information.

February 3, 2026

Energy-Driven Radius Evolution of Chthonian Planets: A Viscoelastic Maxwell Framework with Applications to Earth

J. Mestan[a,*]

[a] *TerraMakers, Jaroslava Svehly 1435, Prague-Zbraslav, 15600, Czechia*

Abstract

Chthonian planets—dense rocky or metallic remnants of gas giants stripped of their gaseous envelopes—experience extreme internal pressures and energy densities, making their structural evolution fundamentally different from classical terrestrial planets. We aim to develop a physically grounded framework to describe energy-driven radius evolution in such bodies and to understand how internal properties control their structural changes. Using mass conservation, hydrostatic equilibrium, and the virial theorem, we link changes in internal energy to gravitational potential energy. A single-mode Maxwell viscoelastic model is applied to derive an analytically solvable law for quasi-static radius relaxation. Earth is used as a case study to estimate effective interior viscosities and energy transformations during hypothetical historical expansion. Ultra-compressed interiors resist rapid expansion, while structural adjustments or reductions in viscosity can transiently accelerate radius growth. The model quantifies the influence of internal energy reservoirs on radius evolution and highlights the characteristic viscoelastic timescale of global

*Corresponding author.
Email address: info@terramakers.com (J. Mestan)

relaxation. This framework provides a transparent and falsifiable model connecting microphysical planetary properties to macroscopic radius evolution, offering predictive insights for both Earth and exoplanetary chthonian cores.

Keywords: chthonian planets, planetary radius evolution, energy conservation, viscoelastic relaxation, Maxwell rheology, internal energy

---

Abbreviations

EOS Equation of State

GBE Gravitational Binding Energy

GPS Global Positioning System

LOD Length of Day

WDM Warm Dense Matter

1. Introduction

Chthonian planets represent a unique class of rocky or metallic bodies, thought to originate as the dense cores of gas giants that have lost their primordial gaseous envelopes through intense stellar irradiation and photoevaporation [1, 12, 31]. While some studies indicate that many high-density exoplanets may not be remnants of giant-planet cores [21], these objects are nonetheless distinguished by their high mean densities, extreme internal pressures, and thermodynamic properties that differ fundamentally from those of terrestrial planets formed classically. With ongoing observational surveys—particularly mass/density–radius studies of exoplanets [26]—continuing to

uncover compact, high-density worlds, investigating the long-term structural and mechanical evolution of these bodies has become increasingly crucial.

The extreme pressures experienced during formation result in the accumulation of internal energy across multiple channels. As a chthonian planet evolves and cools, this energy may be gradually redistributed and converted into gravitational potential energy, potentially driving slow radial expansion (Fig. 1). Despite its relevance for interpreting observed exoplanet radii and densities, this energy-driven expansion has not yet been formulated in a simple, physically transparent, and quantitatively predictive framework.

Early investigations of planetary relaxation employed viscoelastic models, most notably the Maxwell rheological framework applied to the relaxation of a homogeneous self-gravitating sphere [25]. These studies demonstrated that, depending on volumetric strain, relaxation timescales may range from rapid adjustment to processes extending over billions of years. In the regime of extremely high viscosity expected for ultracompressed planetary interiors, expansion proceeds as a slow, quasi-static process governed by long relaxation times.

Beyond exoplanets, Earth provides a unique natural laboratory in which radius evolution can, in principle, be constrained by geological and geodetic observations. The hypothesis that Earth may have experienced radial expansion has a long history [3]. Early work by Hilgenberg [15] approached the problem geometrically, reconstructing the Earth's surface to accommodate changes in planetary volume, while Halm [9] introduced a dynamical perspective in which Earth's radius increased over time, leading to a gradual decrease in mean density. Later descriptive frameworks, such as Whole Earth

Decompression Dynamics [14], further explored these concepts, emphasizing large-scale crustal rearrangements without relying on detailed physical assumptions. More recently, structural and geometric analyses have explored the novel possibility that Earth could represent a limiting case of a chthonian planet that has undergone partial relaxation following the loss of an early massive gaseous envelope [23]. While these ideas remain controversial, they motivate the development of a physically grounded framework capable of quantitatively assessing whether energy-driven expansion is plausible under realistic material and dynamical constraints.

In this work, we derive an effective relation governing the radius evolution of chthonian planets from first principles, including mass conservation, hydrostatic equilibrium, and the virial theorem. By explicitly linking changes in internal energy to GBE, we obtain a closed, first-order law describing the global relaxation of planetary radius toward an equilibrium value on a characteristic Maxwell viscoelastic timescale. The resulting formulation is analytically tractable, requires only a small number of physically interpretable parameters, and can be generalized to include effective viscoelastic weakening during expansion. The framework is then applied to Earth as an illustrative case, allowing order-of-magnitude estimates of internal energy transformation and effective interior viscosity over geological timescales.

2. Internal Energy and Pressure in Ultracompressed Planetary Matter

2.1. Contributions to Internal Energy

The internal energy of a dense planetary core originates from its formation as the central region of a gas giant and from subsequent early evolution. During any later expansion, a fraction of this energy is gradually converted into gravitational potential energy, rendering the GBE less negative. Expansion occurs through mechanical work done by internal pressure against self-gravity and its rate is moderated by the viscoelastic behavior of the planetary interior.

In ultracompressed planetary materials, the internal energy can be decomposed into distinct physical contributions:

- **Thermal energy**, associated with the kinetic motion of ions and atoms
- **Coulomb energy**, arising from electrostatic interactions between nuclei and electrons (including exchange and correlation effects)
- **Electron kinetic energy**, comprising the kinetic energy associated with Fermi degeneracy at high electron density, as well as thermal excitations of the electron gas
- **Elastic energy**, due to compression and deformation of the material in solid or superionic phases
- **Phase and chemical energy**, associated with structural rearrangements, ionization, and phase transitions (solid, liquid, superionic)

Thus, the total internal energy is

$$E_{\text{internal}} = E_{\text{thermal}} + E_{\text{Coulomb}} + E_{\text{electron}} + E_{\text{elastic}} + E_{\text{phase}} \,. \tag{1}$$

While these contributions provide a useful framework, they are often coupled and can overlap under extreme conditions, as electronic and ionic motions, lattice deformations, and phase changes influence each other. It is also important to note that magnetic energy, radiation energy, relativistic corrections, and neutrino energy losses may also contribute to the internal energy, although they are generally secondary and often negligible compared to the primary selected contributions.

In the deep interiors of gas giants and chthonian planets, matter may exist in the WDM regime or a supercompressed state [8]. Typical WDM conditions involve densities up to $\sim 10^2$ g cm^{-3} and temperatures in the range 1–100 eV [6]. In this regime, matter is partially ionized and occupies an intermediate state between condensed matter and fully ionized plasma. At these densities—much lower than those of white dwarfs or neutron stars [13]—electron degeneracy pressure is subdominant, though non-negligible. Interatomic distances in such conditions are strongly reduced, discrete atomic shells are largely suppressed, and the material behaves as a strongly coupled ionic fluid embedded in a partially delocalized electron background. Under these circumstances, materials may acquire metallic properties even if insulating under ambient conditions [7].

The thermodynamic and mechanical behavior of ultracompressed planetary matter is thus governed by the combined effects of thermal motion, Coulomb interactions, electron kinetic energy acquired by electrons under strong electronic confinement, elastic deformation, and phase transitions.

The relative weight of each contribution depends on local density, temperature, composition, ionization state, and electronic structure.

2.2. Contributions to Internal Pressure

Analogous to the internal energy decomposition, the total internal pressure can be written as

$$P_{\text{internal}} = P_{\text{thermal}} + P_{\text{Coulomb}} + P_{\text{electron}} + P_{\text{elastic}} + P_{\text{phase}}\,. \tag{2}$$

Hydrostatic pressures in the deep interiors of gas giants reach the terapascal (TPa) range; for example, pressures at Jupiter's center may approach $\sim 7\,\text{TPa}$ [27]. The Coulomb and electron kinetic contributions provide the fundamental microscopic pressure required to sustain hydrostatic equilibrium against the planet's self-gravity. In the ultracompressed regime, these terms dominate the EOS, effectively defining the total pressure at every depth.

During the formation of a chthonian planet, overlying mass is lost and hydrostatic pressure may drop by several TPa. Nevertheless, internal material pressures remain approximately constant until the interior begins to expand or lose some energy, mainly by radiation to space. Planetary expansion proceeds only if the combined internal pressures exceed the reduced hydrostatic pressure; otherwise, the core remains largely unchanged in radius.

3. Mass Conservation and Radius Evolution

Mass conservation imposes a fundamental geometric constraint linking the planetary radius to its mean density. For a spherical planet of mass M, radius R, and mean density $\bar{\rho}$, the relation is

$$M = \frac{4}{3}\pi R^3 \bar{\rho}\,. \tag{3}$$

For a chthonian planet undergoing expansion, the total mass is conserved:

$$\frac{dM}{dt} = 0\,, \tag{4}$$

which directly implies

$$\frac{d}{dt}\left(\bar{\rho}R^3\right) = 0\,. \tag{5}$$

Consequently, any increase in the planetary radius must be accompanied by a corresponding decrease in mean density. This constraint establishes the geometric foundation for energy-driven radius evolution and provides a direct link between internal energy redistribution and macroscopic structural change.

4. Hydrostatic Structure and the Virial Relation

Assuming spherical symmetry and negligible rotation, the mass enclosed within radius R is

$$M = \int_0^R 4\pi r^2\,\rho(r)\,dr\,. \tag{6}$$

Hydrostatic equilibrium requires

$$\frac{dP}{dr} = -\frac{Gm(r)\,\rho(r)}{r^2}\,, \tag{7}$$

where P is the local pressure and G is the gravitational constant.

The GBE of the planet is

$$U_{\rm GBE} = -\int_0^R \frac{Gm(r)}{r}\,dm(r)\,. \tag{8}$$

Multiplying Eq. (7) by $4\pi r^3 dr$ and integrating over the planetary radius yields the one-dimensional virial relation:

$$U_{\rm GBE} + 3\int_0^R 4\pi r^2 P(r)\,dr = -4\pi R^3 P(R)\,. \tag{9}$$

For an isolated planet, the surface pressure is negligible, $P(R) \sim 0$, giving

$$U_{\mathrm{GBE}} = -3 \int_0^R 4\pi r^2 P(r)\, dr\,. \tag{10}$$

This relation can be expressed in the compact form

$$U_{\mathrm{GBE}} = -a\,\frac{GM^2}{R}\,, \tag{11}$$

where a is a dimensionless structure factor determined by the internal mass distribution.

5. Effective Expansion Relation for a Chthonian Planet

Energy conservation implies that changes in the internal energy are balanced by changes in GBE:

$$\frac{dE_{\mathrm{internal}}}{dt} = -\frac{dU_{\mathrm{GBE}}}{dt}\,. \tag{12}$$

Using the compact form $U_{\mathrm{GBE}} = -aGM^2/R$, the time derivative becomes

$$\frac{dE_{\mathrm{internal}}}{dt} = -a\frac{GM^2}{R^2}\frac{dR}{dt}\,. \tag{13}$$

This yields the effective expansion relation:

$$\frac{dR}{dt} = -kR^2\frac{dE_{\mathrm{internal}}}{dt}\,, \tag{14}$$

where

$$k = \frac{1}{aGM^2}\,. \tag{15}$$

Eq. (14) provides a direct quantitative link between internal power and planetary radius growth. In this formulation, the structure factor a is assumed constant, corresponding to homologous expansion with a self-similar

internal density profile. In nature, one can expect non-homologous behavior accompanied by mass redistribution and changes in the moment of inertia of the planet. Consequently, the power required for expansion will likely not remain constant but will vary, increasing and decreasing over time.

6. Effective Law of Chthonian Planet Expansion

The expansion of a chthonian planet can be described by a minimal effective law based on a single viscoelastic relaxation mode. In this framework, the internal energy stored in compressional deformation relaxes over a characteristic Maxwell timescale τ, driving changes in the planetary radius.

6.1. Maxwell Relaxation

We define the excess energy relative to equilibrium as

$$E_{\text{excess}}(R) = aGM^2 \left(\frac{1}{R} - \frac{1}{R_{\text{eq}}} \right), \tag{16}$$

where E_{excess} represents the stored compressional energy driving expansion and R_{eq} is the relaxed equilibrium radius.

The internal energy evolves according to a Maxwell-type relaxation:

$$\frac{dE_{\text{internal}}}{dt} = -\frac{E_{\text{excess}}(R)}{\tau}, \tag{17}$$

where the characteristic Maxwell time required for stored compressional energy to be converted into gravitational potential energy through viscous flow is

$$\tau = \frac{\eta}{E}, \tag{18}$$

with η the effective viscosity and E the effective elastic modulus of the planetary interior. The effective viscosity represents an effective macroscopic viscosity controlling the rate of global volumetric relaxation of the planet, not a local shear viscosity. It averages over pressure, temperature, phase state, and microstructural damage. The effective elastic modulus characterizes the global resistance of the self-gravitating planet to volumetric deformation and incorporates both material compressibility and gravitational confinement.

6.2. Closed Radius Evolution Law

Substituting Eq. (17) into the effective expansion relation (14) gives the single-mode Maxwell radius evolution law:

$$\frac{dR}{dt} = \frac{R^2}{\tau}\left(\frac{1}{R} - \frac{1}{R_{\rm eq}}\right) = \frac{R}{\tau}\left(1 - \frac{R}{R_{\rm eq}}\right). \tag{19}$$

6.3. Analytical Solution

The solution of Eq. (19) for an initial radius R_0 is

$$R(t) = \frac{R_{\rm eq}}{1 + \left(\frac{R_{\rm eq}}{R_0} - 1\right) e^{-t/\tau}}, \tag{20}$$

which exhibits the expected behavior:

- Rapid expansion at early times when $R \ll R_{\rm eq}$
- Slower growth as R approaches $R_{\rm eq}$
- Asymptotic approach to $R_{\rm eq}$, naturally shutting off further expansion

6.4. Viscoelastic Weakening and Accelerated Expansion

In realistic planetary interiors, viscosity may decrease as pressure is relieved during expansion. This can be incorporated by allowing the Maxwell time to depend on radius:

$$\tau(R) = \frac{\eta(R)}{E}\,, \tag{21}$$

leading to a generalized radius evolution law:

$$\frac{dR}{dt} = \frac{R}{\tau(R)}\left(1 - \frac{R}{R_{\rm eq}}\right). \tag{22}$$

If $\tau(R)$ decreases sufficiently with increasing R, the expansion rate can accelerate over a finite interval, providing a natural mechanism for transient runaway expansion without introducing additional dynamical degrees of freedom.

6.5. Physical Interpretation

This effective law captures the essential physics of chthonian planet expansion: the planet relaxes toward an equilibrium radius on a Maxwell timescale, converting excess compressional energy into gravitational potential energy. It provides a transparent, falsifiable, and quantitatively predictive framework for radius evolution without requiring arbitrary parameters or multiple relaxation modes. In this formulation, the Maxwell timescale $\tau = \eta/E$ should be understood as an effective relaxation parameter. A reduction of τ may reflect not only a decrease in the intrinsic viscosity η of planetary materials, but equally an increase of the effective elastic rigidity E due to structural reorganization or phase transitions. These effects lower the planet's macroscopic resistance to deformation even when local material viscosities remain extremely high. The single-mode Maxwell law can be

interpreted as the dominant-mode limit of a more complex, multi-layer viscoelastic interior, justifying its use as a physically grounded effective model for chthonian planet expansion.

7. Mechanical and Rheological Conditions for Expansion

The expansion of a chthonian planet is fundamentally governed by the balance between internal mechanical forces and self-gravity. Conceptually, expansion occurs when internal pressure is sufficient to overcome gravitational confinement and perform the work required to displace overlying material. Mathematically, the condition for expansion can be expressed as

$$P_{\text{internal}} \gtrsim P_{\text{gravity}} \,, \tag{23}$$

where P_{internal} is the effective internal pressure defined by Eq. (2), and P_{gravity} is the cumulative gravitational pressure from overlying layers.

A practical estimate of the local gravitational pressure at radius r is

$$P_{\text{gravity}}(r) = \int_r^R \rho(r')\, g(r')\, dr' \,, \tag{24}$$

with $\rho(r')$ the local density, $g(r')$ the gravitational acceleration, and R the total planetary radius. This integral represents the overburden pressure that must be overcome for expansion at a given depth $R - r$.

Even when internal pressure locally exceeds gravitational confinement, the rate of expansion is strongly limited by the planet's rheology. A high-viscosity interior resists flow, so expansion proceeds on long, viscoelastic timescales rather than rapidly. In the present framework, this behavior is captured by the Maxwell relaxation time τ, and the resulting expansion is

described by the single-mode radius evolution law (19). Planetary expansion requires, given the excess internal energy E_{excess}, that (a) internal pressures exceed self-gravity, and (b) the interior can deform on the appropriate viscoelastic timescale. Furthermore, transient changes in material properties—such as viscoelastic changes due to decompression or phase transitions—can locally accelerate expansion, as captured by a radius-dependent Maxwell time $\tau(R)$.

8. Principle of Chthonian Planet Expansion

The effective expansion relation (14) encapsulates a fundamental principle governing the long-term evolution of highly compressed planetary bodies:

> Chthonian planets expand through the progressive transformation of internal energy into gravitational potential energy, subject to mass conservation, self-gravity, and the viscoelastic properties of the interior.

This principle highlights the core mechanisms controlling planetary radius evolution:

- **Energy transformation:** Excess internal energy stored in the planet is converted into gravitational potential energy, driving an increase in radius.
- **Gravitational confinement:** Expansion occurs only when internal pressures exceed the cumulative gravitational pressure from overlying layers.

- **Viscoelastic modulation:** The interior viscosity sets the timescale of expansion. Regions of high viscosity relax slowly, limiting radial growth, whereas viscosity reduction can transiently accelerate expansion.

- **Equilibrium radius:** The planet evolves toward a characteristic equilibrium radius R_{eq}, determined by the balance between internal energy, gravitational binding, and structural properties. The approach is governed by the Maxwell relaxation timescale $\tau = \eta/E$.

Overall, this principle provides a physically grounded framework linking the microphysics of planetary interiors to macroscopic radius evolution. It justifies the use of a single-mode Maxwell law (19) as a minimal, analytically tractable model for chthonian planet expansion, while remaining extensible to more complex, multi-layered interiors. By formalizing this concept, one can predict and interpret the long-term radius evolution of highly compressed terrestrial bodies, including potential applications to Earth-like planets.

9. Application to Earth

9.1. Two Mechanical Eras

Earth is estimated to have formed approximately 4.56 Ga [11], likely at an orbital position differing from its current location, consistent with possible early planetary migration [4, 32]. The detailed trajectory and timing of Earth's migration remain an open question. Lammer et al. [19] suggest that planetary embryos exceeding $\sim 0.5\,M_{\oplus}$ prior to protoplanetary disk dispersal accrete substantial primordial H_2-rich atmospheres. In contrast, late-stage

terrestrial formation occurs after the dissipation of the gaseous disk, producing planets with comparatively thin atmospheres. Zircon evidence for felsic crust older than 4.0 Gyr [10] indicates that early surface pressures were far below the TPa regime, consistent with substantial atmospheric loss in the proto-Earth. Within this framework, we hypothesize that Earth initially formed as the core of a gas-giant-like planet and subsequently lost most of its hydrogen–helium envelope via photoevaporation over the first $\sim 10^7$–10^8 yr. Following envelope removal, the proto-Earth would have been significantly denser and more compact, with a radius of $\sim 0.55\,R_\oplus$ or smaller.

In the context of the Earth expansion hypothesis [3, 15], the chthonian planet's evolution can be conceptually divided into two mechanical eras:

- From chthonian formation to approximately 200 Myr ago, corresponding to the primary phase of radius expansion
- The subsequent $\sim$ 200 Myr interval, during which surface and lithospheric dynamics dominated, reflecting the subsequent stages of expansion (Fig. 2)

By restoring the Earth to its size around 200 million years ago—when oceanic crust was minimal and the surface was almost entirely continental—it becomes possible to fit together not only Africa with South America, as proposed originally by Wegener [35] for the continental drift and non-expanding Earth scenario, but also South America with Zealandia (Fig. 3), as proposed by Mestan [23] for the expanding Earth scenario.

Limited expansion during the initial mechanical era likely produced negligible new oceanic crust, leaving little direct geological record. During a

subsequent mechanical era, Earth may have expanded substantially, increasing its volume by a factor of ~ 6 over ~ 200 Myr. This expansion reduced the mean density to near-modern values and lowered surface gravity, as illustrated schematically in Fig. 4.

Throughout both mechanical eras, the effective viscosity of Earth's interior materials must have been exceptionally high. As summarized in Table 1, the estimated parameters for the chthonian Earth 200 Myr ago are extreme, yet not unprecedented when compared with exoplanetary bodies. For example, the density of Kepler-52 c is estimated at 3.63×10^4 kg m^{-3}, Kepler-52 b at 5.06×10^4 kg m^{-3} [25], and GP Com b may reach 1.88×10^5 kg m^{-3} [18], possibly containing strange quark matter. Such extreme densities naturally correspond to extreme parameters, including surface gravity and central hydrostatic pressure.

9.2. Earth's Radius Evolution Modeling

Analyses of oceanic crust formation data over the past 338 Myr [29] suggest—within the framework of the hypothetical planetary expansion scenario—that Earth has not yet attained its equilibrium radius and may still be undergoing radial growth (Fig. 5). Several qualitative evolutionary pathways are consistent with the available data: the expansion rate may accelerate, potentially due to a reduction in effective viscosity; proceed approximately linearly; or decelerate as equilibrium is approached. In all cases, however, the long-term evolution is expected to asymptotically converge toward a characteristic equilibrium radius.

To compare the observationally inferred radius evolution with the simplified Maxwell relaxation model, we estimated the inflection behavior of the

dataset (Fig. 6) by computing its second derivative. The substantial variability and noise inherent in the data preclude identification of a unique inflection point; at best, a broad region—or multiple candidate inflection intervals—can be inferred. It should be emphasized that this analysis accounts solely for radius growth associated with oceanic crust formation. In reality, the planetary radius would also increase, albeit more modestly, due to lateral extension of continental crust.

Within the proposed model (Fig. 7), the viscoelastic relaxation time $\tau(t)$ is assumed to change discontinuously at $t = -200$ Myr, corresponding to a transition between two mechanical regimes characterized by distinct effective viscosities. Prior to this epoch, the relaxation time is constant and denoted $\tau_{\text{first era}}$, while for $t \geq -200$ Myr it is replaced by a shorter relaxation time $\tau_{\text{second era}}$. This prescription is expressed as the following piecewise relation:

$$\tau(t) = \begin{cases} \tau_{\text{first era}}, & t < -200 \text{ Myr}, \\ \tau_{\text{second era}}, & t \geq -200 \text{ Myr}. \end{cases} \tag{25}$$

The early-time relaxation parameter $\tau_{\text{first era}}$ is assumed, while $\tau_{\text{second era}}$ is inferred by fitting the model to the inferred planetary radius at $t = -200$ Myr. The reduction in relaxation time is interpreted as a consequence of viscoelastic weakening, potentially driven by decompression, phase transitions, or structural reorganization of the deep interior. An example of a zone exhibiting an extreme viscosity drop in the present-day Earth is the solid–liquid phase transition layer at the inner-core boundary (ICB).

The system is allowed to relax toward equilibrium over 4.36 Gyr, evolving from an initial test radius of 3300 km to approximately 3504 km at -200 Myr.

Thus the initial model time for R_0 is set to -4.56 Gyr; nevertheless, relaxation may have commenced somewhat later, after the gas giant was fully formed and began to lose mass through photoevaporation. Following the inferred viscoelastic reduction, radial expansion accelerates toward equilibrium. At a test $R_{\rm eq}$ value of 6686 km, the corresponding mean density decreases to $4.77 \times 10^3\,\mathrm{kg\,m^{-3}}$. This value is intermediate between the present-day mean densities of Venus ($5.24 \times 10^3\,\mathrm{kg\,m^{-3}}$) and Mars ($3.94 \times 10^3\,\mathrm{kg\,m^{-3}}$) [34]. Present-day Earth is the planet with the highest mean density in the Solar System. Adopting a range of representative effective elastic moduli appropriate for high-pressure planetary interiors, we derive three corresponding estimates of effective viscosity for both mechanical eras. These values are summarized in Table 2.

Given the exceedingly long relaxation times inferred for the early mechanical era, the interior material behaves as effectively locked, exhibiting negligible stress relaxation over the 4.36 Gyr timescale. Even adopting the lowest elastic modulus considered (0.36 TPa), the resulting effective viscosities of order $10^{29}\,\mathrm{Pa\,s}$ are extraordinarily large, far exceeding viscosities measured in laboratory experiments, inferred for natural terrestrial materials, or estimated for Earth's upper mantle [30]. Such values approach those inferred for extreme astrophysical environments in which degeneracy pressure strongly influences material behavior, reinforcing the interpretation of Earth's deep interior as a region characterized by hypothetically exceptional effective (paleo)viscosity. For comparison, viscosities as high as $10^{40}\,\mathrm{Pa\,s}$ have been reported in the literature for glass at room temperature, implying a material that is effectively solid on any observable timescale, with macroscopic flow

rendered negligible [2]. In contrast, the viscosities inferred for the second mechanical era are substantially lower and lie much closer to the 10^{25} Pa s values adopted by Mocquet et al. [25], as well as to viscosities up to 10^{26} Pa s obtained from ab initio numerical simulations of mantle dynamics under the extreme pressures and temperatures characteristic of super-Earth interiors [33].

A central question in planetary evolution (Fig. 8) is why Earth remained largely non-expanding, or expanding only minimally, for over 4 Gyr, followed by a phase of rapid expansion in which planetary volume increased by approximately a factor of ~ 6. Possible mechanisms that warrant further investigation include:

- Structural factors related to phase transitions (e.g., solid–liquid) or evolving core–mantle interactions
- Progressive heterogeneous cooling of the metastable, ultracompressed planetary interior, combined with the development of locally distributed stresses
- The presence of surface ice layers possibly acting as an effective thermal insulator over geological timescales, keeping the interior of the planet hot

9.3. Exploring Internal Energy at the Atomic Scale

If Earth underwent relaxation in the manner proposed, it becomes necessary to identify the microscopic source of the energy driving this process. Owing to the astronomical number of constituent particles, it is neither feasible nor meaningful to track individual interactions directly. Instead, a

coarse-grained approach can be adopted in which the total number of atoms in the Earth is estimated and a representative mean energy contribution is assigned to each atom, corresponding to the energy acquired during compression in a hypothesized gas giant evolutionary stage. While Earth materials exhibit a wide range of bonding environments, the present calculation does not assume uniform microscopic behavior.

At the extreme pressures of planetary interiors, distinctions between metallic, ionic, and covalent bonding become increasingly blurred and the parameter $E_{\text{excess}}(R_0)$ from (16) divided by the number of atoms provides a characteristic mean energy scale, rather than a precise per-atom value. The purpose of this estimate is therefore not to model specific bonding mechanisms, but to demonstrate that the characteristic microscopic energy scale required to account for global planetary relaxation is comparable to known chemical and lattice energies. The cumulative contribution of these atomic-scale energies should approximately match the change in Earth's GBE associated with planetary relaxation. In this framework, even minute changes in interatomic spacing or local volume at the microscopic level contribute collectively to the macroscopic energy budget governing planetary expansion. The compositional basis for this estimate is summarized in Table 3, which shows that Earth's bulk composition is dominated by a small number of elements, principally Fe, O, Si, and Mg.

Using the compositional data from Table 3 and the Earth's mass from Table 1, we can estimate the total number of atoms in the planet. Assuming a mean atomic mass of ≈ 26.26 u (standard atomic weights of elements taken from [28]), the mass per atom is

$$M_{\text{atom}} \approx 4.36 \times 10^{-26} \text{ kg}. \tag{26}$$

Consequently, the total number of atoms in the Earth is

$$\frac{M_{\oplus}}{M_{\text{atom}}} \approx 1.37 \times 10^{50}. \tag{27}$$

The energy released during the hypothesized planetary relaxation is on the order of 10^{32} J. Dividing by the total number of atoms yields a mean energy per atom of

$$\frac{10^{32} \text{ J}}{1.37 \times 10^{50}} \approx 7.30 \times 10^{-19} \text{ J}. \tag{28}$$

Expressed in electronvolts, this corresponds to

$$E_{\text{gain}} = \frac{7.30 \times 10^{-19} \text{ J}}{1.60 \times 10^{-19} \text{ J/eV}} \approx 4.56 \text{ eV}. \tag{29}$$

This value is consistent with typical chemical bonding energies in solids, which generally range from 1–10 eV [20], depending on the element and bond type. Cohesive and lattice energies of Earth's materials provide a comparable scale. The first ionization energy, approximately 10.74 eV per atom (Table 3), also provides a characteristic energy scale consistent with computed value. From this perspective, the planetary interior cannot remain molecular because the net energy gain—driven by the excess of electron kinetic energy—surpasses the molecular binding threshold, forcing a transition into a metallic state [7].

The atomic binding energy reservoir imposes a fundamental constraint on planetary compression and expansion. Planetary matter strongly resists uniform compression; in the case of Earth, overcoming this barrier requires total

energies on the order of 10^{32} J, corresponding to $\sim +5$ eV net gain/atom. The net microscopic energy gain E_{gain} integrated over whole Earth (27) corresponds to the excess energy term $E_{\text{excess}}(R_0)$ in (16), representing stored compressional energy driving Earth-scale relaxation. On the planetary scale, the exchange between this excess energy and gravitational potential energy is captured by the Maxwell viscoelastic relaxation framework (19).

10. Discussion

10.1. Interpretation and Implications

Expansion driven by internal energy is plausible: excess energy stored in Coulomb, phase-transition, and fermionic degrees of freedom can, in principle, overcome gravitational confinement and increase planetary radius toward equilibrium. The rate of expansion, however, is controlled by the effective viscosity of the interior, so ultra-compressed, high-viscosity cores evolve only slowly over geological timescales. Transient acceleration may occur when the Maxwell timescale decreases due to decompression, phase transitions, or structural reorganization. Earth provides a case study: if historical expansion took place, inferred effective viscosities would have been exceptionally high, consistent with the slow relaxation of an ultra-dense chthonian core. Observational proxies—including geodetic measurements indicating radius growth of $\sim$ 10–20 mm yr^{-1} and a positive effect in ΔLOD of $\sim 0.X$ ms yr^{-1}, as well as reconstructions of oceanic crust growth—may provide indirect evidence.

10.2. Limitations

The single-mode Maxwell approximation captures only the dominant relaxation behavior, whereas multi-layered interiors with heterogeneous viscosi-

ties may exhibit multi-timescale responses. Several secondary processes—including tidal interactions, planetary rotation, centrifugal forces, differentiation, and energy loss to space—are not explicitly included; while these factors can modulate expansion, they are expected to be secondary relative to the primary energy-driven mechanism. Uncertainties in the pressure, viscosity, and elastic moduli of Earth's deep interior and exoplanetary cores further limit the precision of quantitative predictions.

10.3. Future Directions

Long-term, high-precision GPS measurements [24] and paleogeophysical reconstructions [23, 29] could detect subtle or historical changes in Earth's radius, providing empirical tests of predicted expansion rates. However, variability in Earth's rotation caused by general mass redistributions complicates the use of ΔLOD data for inferring planetary expansion. Multi-layer viscoelastic simulations that incorporate realistic EOS, phase transitions, and viscosity variations could refine single-mode Maxwell predictions and assess the impact of heterogeneous interiors. Observations of ultra-dense chthonian exoplanets [16] may independently test this framework, with bulk density measurements, radius evolution constraints, and stellar irradiation histories providing indirect evidence for energy-driven expansion. Comparative studies within the Solar System—for example, Earth versus Venus, or Earth's topography versus Mars' crustal dichotomy—may reveal analogous processes, although such extensions remain speculative.

11. Conclusion

We have developed a physically grounded framework linking internal energy transformations to the long-term relaxation of chthonian planets via mass conservation, hydrostatic equilibrium, and the virial theorem. By connecting changes in internal energy to gravitational potential energy, a first-order expansion law governed by a Maxwell viscoelastic timescale is derived. Application to Earth suggests that, if radial expansion, originally proposed by Hilgenberg [15], occurred, interior viscosities must have been extremely high, consistent with ultra-compressed, high-density conditions. This framework allows us to estimate such viscosities from radius evolution and demonstrates that the Maxwell timescale reductions can accelerate expansion. The proposed analytical framework assumes that the Earth's hypothetical relaxation is an ongoing present-day process and may be measurable. While simplified, the model captures essential physics of planetary radius evolution and provides a predictive, testable framework for both Earth and exoplanetary chthonian cores. Future work combining geodetic measurements, geological reconstructions, and numerical simulations can test these predictions and probe the viscoelastic behavior of ultra-dense planetary interiors.

References

[1] Armstrong, D.J., Lopez, T.A., Adibekyan, V., 2020. A Remnant Planetary Core in the Hot-Neptune Desert. Nature 583, 39–42. https://doi.org/10.1038/s41586-020-2421-7

[2] Barnes, H.A., Hutton, J.F., Walters, K., 1989. Chapter 2 - Viscosity.

In: An Introduction to Rheology, Rheology Series, vol. 3, pp. 11–35. https://doi.org/10.1016/B978-0-444-87469-6.50006-8

[3] Carey, S.W., 1976. The Expanding Earth. Developments in Geotectonics, vol. 10. Elsevier Scientific Publishing Company, Amsterdam, The Netherlands.

[4] Chrenko, O., Lambrechts, M., 2019. Oscillatory Migration of Accreting Protoplanets Driven by a 3D Distortion of the Gas Flow. Astron. Astrophys. 626, A109. https://doi.org/10.1051/0004-6361/201935334

[5] Dziewonski, A.M., Anderson, D.L., 1981. Preliminary Reference Earth Model. Phys. Earth Planet. Inter. 25, 297–356. https://doi.org/10.1016/0031-9201(81)90046-7

[6] Falk, K., 2018. Experimental Methods for Warm Dense Matter Research. High Power Laser Sci. Eng. 6, e59. https://doi.org/10.1017/hpl.2018.53

[7] Gregoryanz, E., Ji, C., Dalladay-Simpson, P., et al., 2020. Everything You Always Wanted to Know About Metallic Hydrogen but Were Afraid to Ask. Matter Radiat. Extremes 5, 038101. https://doi.org/10.1063/5.0002104

[8] Guillot, T., 1999. Interiors of Giant Planets Inside and Outside the Solar System. Science 286, 72–77. https://doi.org/10.1126/science.286.5437.72

[9] Halm, J.K.E., 1935. An Astronomical Aspect of the Evolution of the Earth (Presidential Address). J. Astron. Soc. South. Afr. 4, 1.

[10] Hastie, A.R., Law, S., Bromiley, G.D., et al., 2023. Deep Formation of Earth's Earliest Continental Crust Consistent with Subduction. Nat. Geosci. 16, 816–821. https://doi.org/10.1038/s41561-023-01249-5

[11] Hazen, R.M., 2010. How Old Is Earth, and How Do We Know? Evo Edu Outreach 3, 198–205. https://doi.org/10.1007/s12052-010-0226-0

[12] Hébrard, G., Lecavelier Des Étangs, A., Vidal-Madjar, A., et al., 2003. Evaporation Rate of Hot Jupiters and Formation of Chthonian Planets. In: Beaulieu, J.-P., Lecavelier des Étangs, A., Terquem, C. (Eds.), Extrasolar Planets: Today and Tomorrow, ASP Conf. Ser., vol. 321, p. 203. https://doi.org/10.48550/arXiv.astro-ph/0312384

[13] Heiselberg, H., Hjorth-Jensen, M., 2000. Phases of Dense Matter in Neutron Stars. Phys. Rep. 328, 237–327. https://doi.org/10.1016/S0370-1573(99)00110-6

[14] Herndon, J.M., 2013. A New Basis of Geoscience: Whole-Earth Decompression Dynamics. arXiv preprint. https://doi.org/10.48550/arXiv.1307.1692

[15] Hilgenberg, O.C., 1933. Vom Wachsenden Erdball. O.C. Hilgenberg, Berlin, Germany.

[16] Houllé, M., Vigan, A., Carlotti, A., et al., 2021. Direct Imaging and Spectroscopy of Exoplanets with the ELT/HARMONI High-Contrast Module. Astron. Astrophys. 652, A67. https://doi.org/10.1051/0004-6361/202140479

[17] Kramida, A., Ralchenko, Yu., Reader, J., et al., 2024. NIST Atomic Spectra Database (ver. 5.12). Available at: https://physics.nist.gov/asd (accessed 31 January 2026).

[18] Kuerban, A., Geng, J.-J., Huang, Y.-F., et al., 2020. Close-In Exoplanets as Candidates for Strange Quark Matter Objects. Astrophys. J. 890, 41. https://doi.org/10.3847/1538-4357/ab698b

[19] Lammer, H., Zerkle, A.L., Gebauer, S., et al., 2018. Origin and Evolution of the Atmospheres of Early Venus, Earth and Mars. Astron. Astrophys. Rev. 26, 2. https://doi.org/10.1007/s00159-018-0108-y

[20] Liao, Y., 2006. Practical Electron Microscopy and Database, An Online Book 3, 1412. Available at: https://www.globalsino.com/EM/page1823.html (accessed 31 January 2026).

[21] Lin, Z., Cambioni, S., Seager, S., 2025. Most High-Density Exoplanets Are Unlikely to Be Remnant Giant Planet's Cores. Astrophys. J. Lett. 978(2), L41. https://doi.org/10.3847/2041-8213/ad86c3

[22] McDonough, W., 2007. Compositional Model for the Earth's Core. In: Treatise on Geochemistry, vol. 2, pp. 547–568. https://doi.org/10.1016/B0-08-043751-6/02015-6

[23] Mestan, J., 2025a. A 3D Rapid Prototyping Method for Visualizing Earth's Expansion Through Handcrafted Models: A Chthonian Planet Perspective. ESS Open Archive. https://doi.org/10.22541/essoar.176005596.61564713/v1

[24] Mestan, J., 2025b. Revisiting GPS-Derived Plate Kinematics: Evaluation of the Integration of Plate Motion Models in Terrestrial Reference Frames. EarthArXiv. https://doi.org/10.31223/x5bj01

[25] Mocquet, A., Grasset, O., Sotin, C., 2014. Very High-Density Planets: A Possible Remnant of Gas Giants. Phil. Trans. R. Soc. A 372, 20130164. https://doi.org/10.1098/rsta.2013.0164

[26] Müller, S., Baron, J., Helled, R., et al., 2024. The Mass-Radius Relation of Exoplanets Revisited. Astron. Astrophys. 686, A296. https://doi.org/10.1051/0004-6361/202348690

[27] Nettelmann, N., Holst, B., Kietzmann, A., et al., 2008. Ab Initio Equation of State Data for Hydrogen, Helium, and Water and the Internal Structure of Jupiter. Astrophys. J. 683, 1217–1228. https://doi.org/10.1086/589806

[28] Prohaska, T., Irrgeher, J., Benefield, J., et al., 2022. Standard atomic weights of the elements 2021 (IUPAC Technical Report). Pure Appl. Chem., 94(5), 573–600. https://doi.org/10.1515/pac-2019-0603

[29] Seton, M., Müller, R.D., Zahirovic, S., et al., 2020. A Global Data Set of Present-Day Oceanic Crustal Age and Seafloor Spreading Parameters. Geochem. Geophys. Geosyst. 21, e2020GC009214. https://doi.org/10.1029/2020GC009214

[30] She, Y., Fu, G., 2019. Viscosities of the Crust and Upper Mantle Constrained by Three-Dimensional GPS Rates in the Sichuan–Yunnan Frag-

ment of China. Earth Planets Space 71, 33. https://doi.org/10.1186/s40623-019-1013-x

[31] Staab, D., Haswell, C.A., Barnes, J.R., et al., 2020. A Compact Multi-Planet System Around a Bright Nearby Star from the Dispersed Matter Planet Project. Nat. Astron. 4, 399. https://doi.org/10.1038/s41550-019-0974-x

[32] Szuszkiewicz, E., Podlewska-Gaca, E., 2012. Migration-Induced Architectures of Planetary Systems. Orig. Life Evol. Biosph. 42, 113–142. https://doi.org/10.1007/s11084-012-9287-0

[33] Tackley, P.J., Ammann, M., Brodholt, J.P., et al., 2013. Mantle Dynamics in Super-Earths: Post-Perovskite Rheology and Self-Regulation of Viscosity. Icarus 225, 50–61. https://doi.org/10.1016/j.icarus.2013.03.013

[34] Taylor, F., Svedhem, H., Head, J., 2018. Venus: The Atmosphere, Climate, Surface, Interior and Near-Space Environment of an Earth-Like Planet. Space Sci. Rev. 214, 35. https://doi.org/10.1007/s11214-018-0467-8

[35] Wegener, A., 1912. Die Entstehung der Kontinente. Geol. Rundsch. 3(4), 276–292. https://doi.org/10.1007/BF02202896

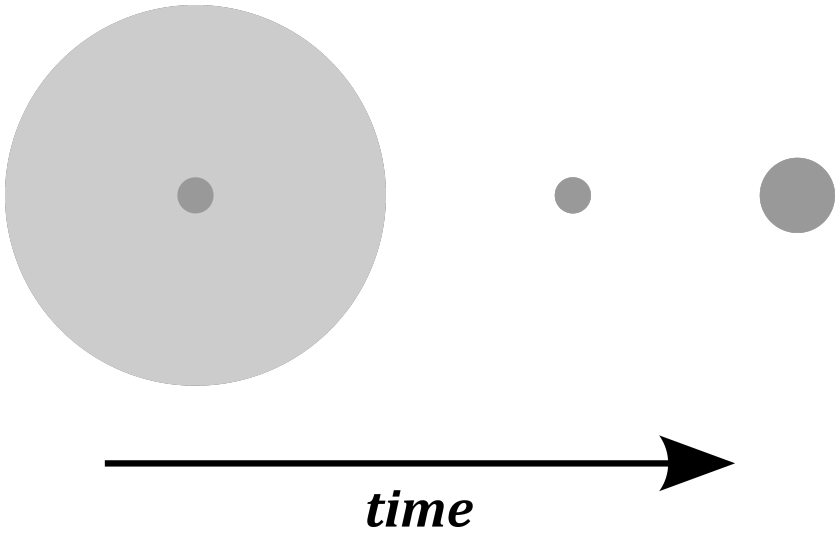

Figure 1: Schematic of the proposed evolution of a chthonian planet: (left) gas giant phase, (center) superdense chthonian core after atmospheric loss, and (right) slowly expanding chthonian planet driven by internal energy redistribution.

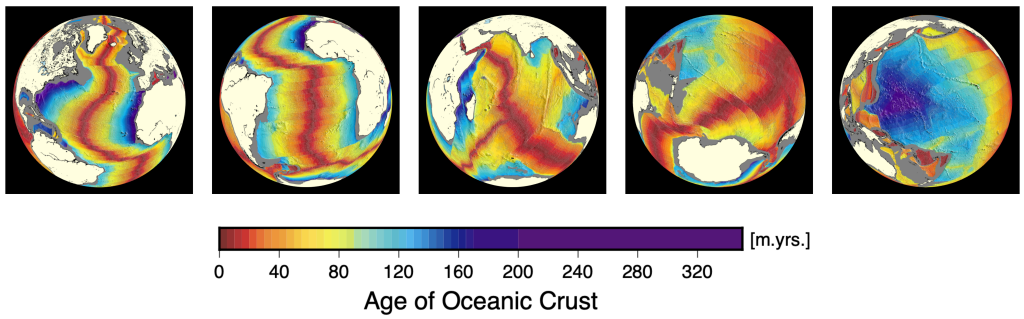

Figure 2: Various views of the Earth showing oceanic crustal ages, predominantly up to approximately 200 Myr. Reproduced from Seton et al. [29].

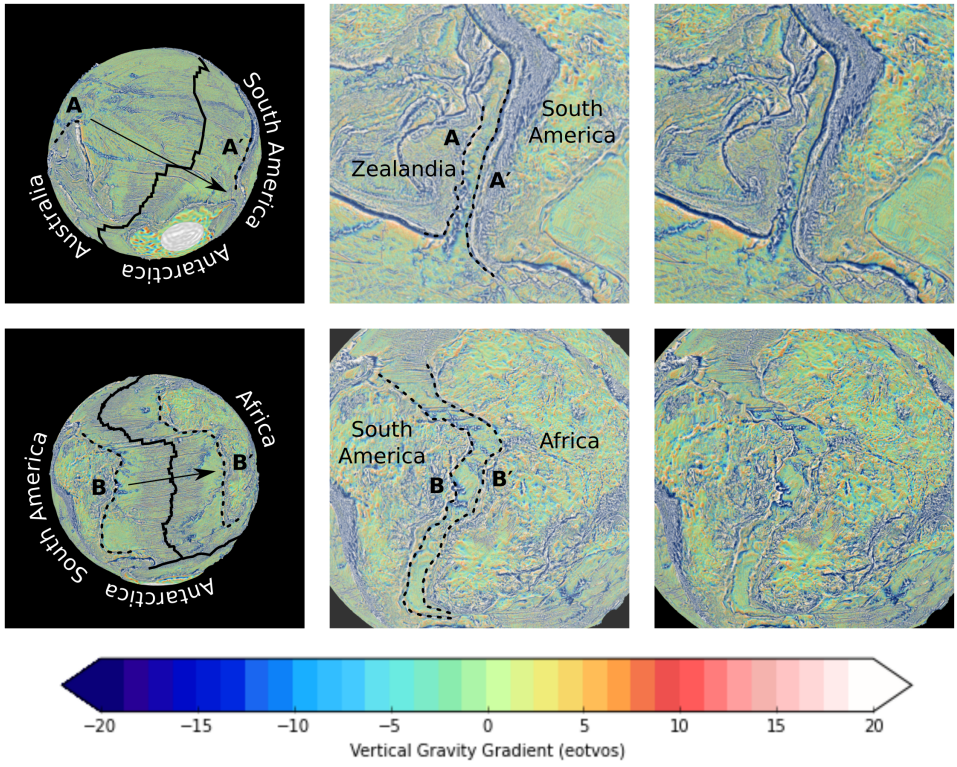

Figure 3: The continental margins of Africa/South America and Zealandia/South America from the 3D vertical gravity gradient model brought into proximity. Solid lines represent the corresponding expansive ruptures, while dashed lines mark the continental margins; the shape similarity is evident. Reproduced from Mestan [23].

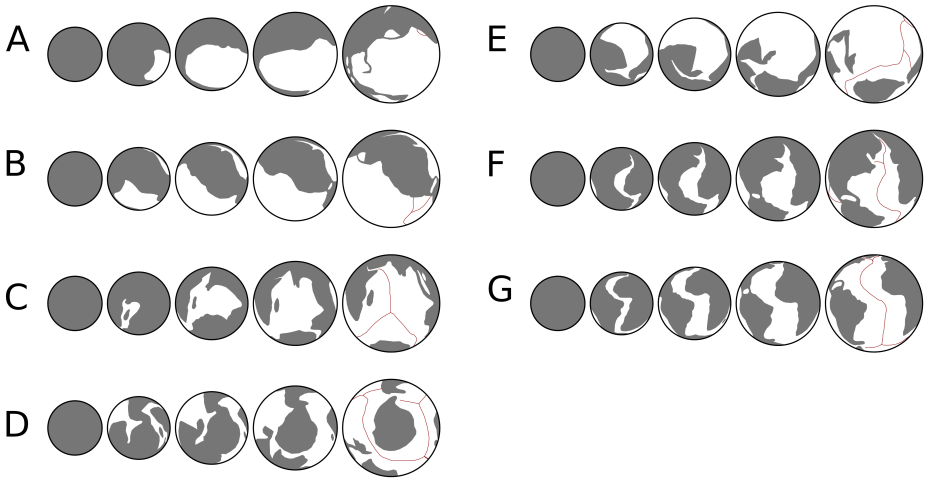

Figure 4: Technical sketches of Earth's expansion ($\sim$ 200 Ma to today), based on rapid prototyping modeling methods, viewed from multiple angles [23]. A: Opening between Eurasia and North America, now occupied by the Pacific Ocean. B: View of North America. C: Divergence between Antarctica and India. D: Expansion in the Antarctic region. E: Separation of Zealandia from South America, with significant deformation of continental crust. F: Spreading near the Mid-Atlantic Ridge between North America and Eurasia. G: Spreading near the Mid-Atlantic Ridge between Africa and South America. Red lines indicate major extensional rupture zones.

Table 1: Comparison of selected calculated physical parameters for the present-day spherical Earth model based on PREM [5] and a hypothesized chthonian Earth 200 Myr ago, including additional expansion parameters. A constant non-uniform structure factor of 0.66 is used for calculation of the GBEs. The ΔLOD estimate assumes uniform radial scaling, conservation of total angular momentum and a moment of inertia factor of 0.33.

Parameter	Recent Earth	Earth 200 Myr Ago
Radius [m]	6.371×10^6	3.504×10^6
Mass [kg]	5.97×10^{24}	5.97×10^{24}
Mean density [$\mathrm{kg\,m^{-3}}$]	5.51×10^3	3.31×10^4
Surface gravity [$\mathrm{m\,s^{-2}}$]	9.82	32.45
Central hydrostatic pressure [TPa]	0.36	$\gg 0.36$
Internal energy transformed [J]	2.02×10^{32}	
Average rate of change of internal energy transformed [W]	3.20×10^{16}	
Average rate of change of radius [$\mathrm{mm\,yr^{-1}}$]	+14.34	
Average rate of change of LOD [$\mathrm{ms\,yr^{-1}}$]	+0.30	

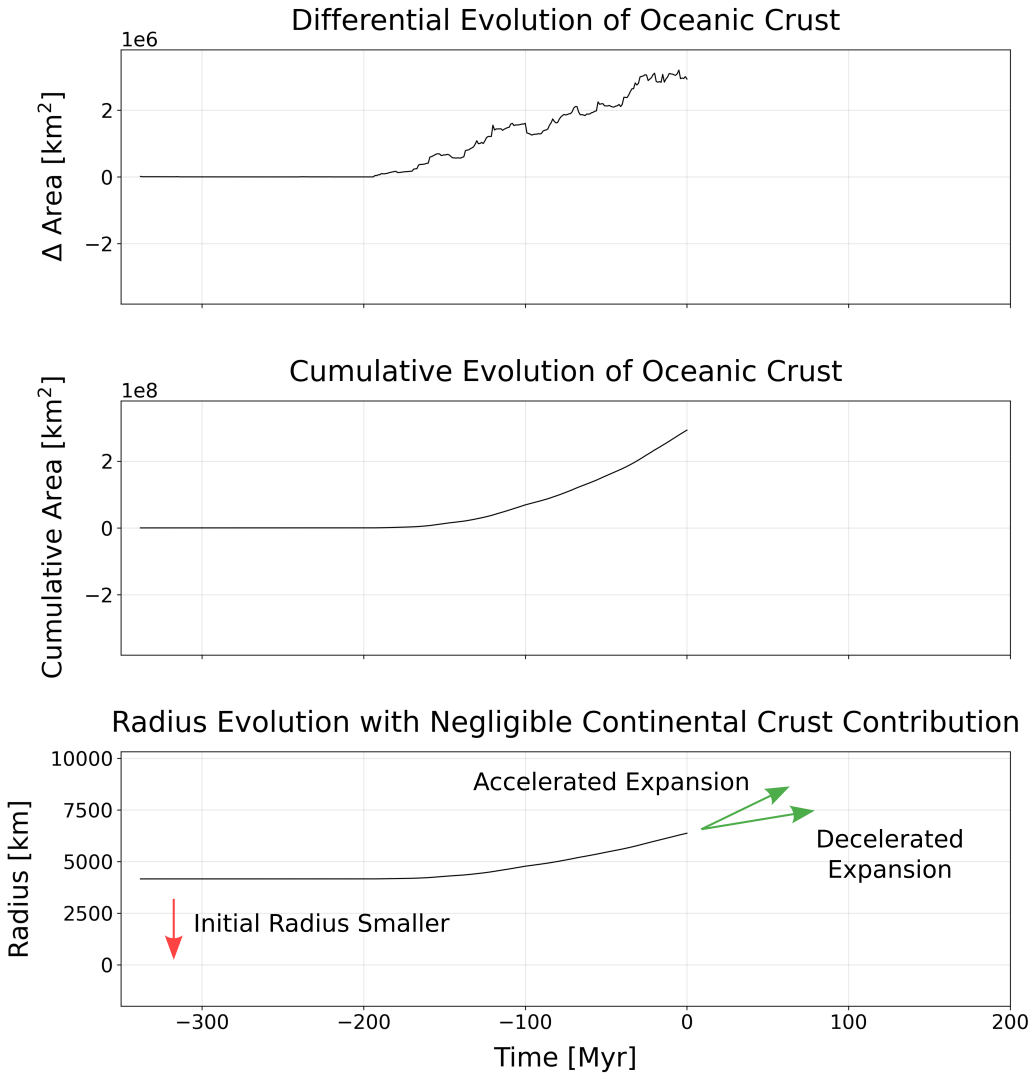

Figure 5: Analysis of oceanic crust formation over the past 338 Myr, based on data from Seton et al. [29]. Under the hypothetical Earth expansion scenario, some regions of continental crust likely increased. Consequently, Earth's original radius may have been significantly smaller than 4157 km, potentially $\sim$ 3504 km at -200 Myr, and possibly even smaller at the time when it existed as a core of a gas giant. Green arrows indicate potential future expansion directions toward equilibrium.

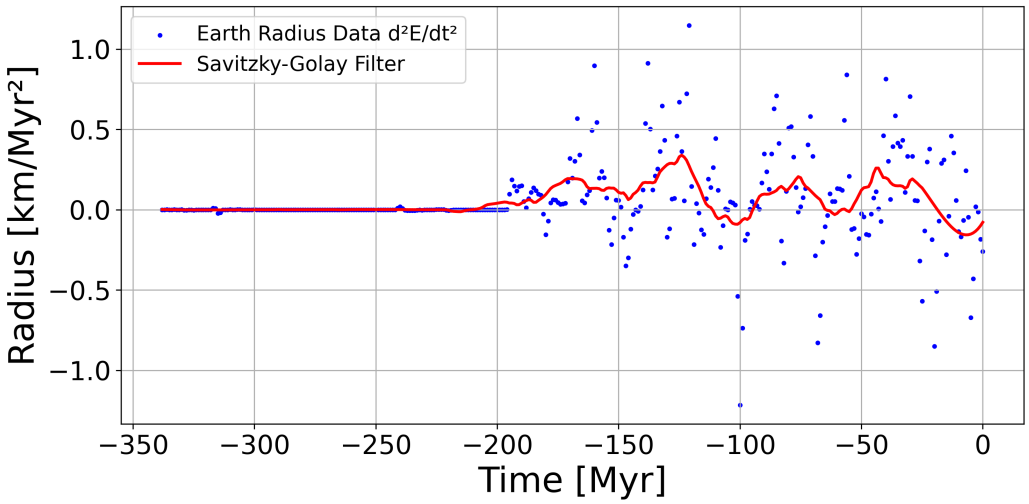

Figure 6: Second derivative of Earth's inferred radius evolution, neglecting lateral extension of the continental crust. While broad curvature changes are apparent, no definitive inflection point can be robustly identified.

Table 2: Model effective elastic moduli and corresponding effective viscosities for the first and second mechanical eras. These values are parameters used in Fig. 7.

E [TPa]	η first era [Pa s]	η second era [Pa s]
0.36	4.0×10^{29}	1.41×10^{27}
0.53	6.0×10^{29}	2.11×10^{27}
0.71	8.0×10^{29}	2.82×10^{27}

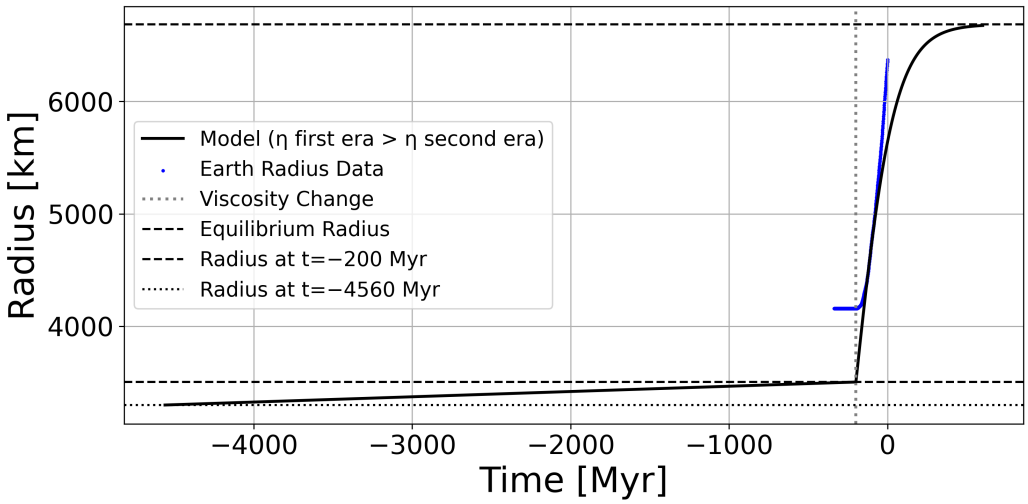

Figure 7: Modeled radial evolution incorporating a time-dependent viscosity characterized by a pronounced decrease around −200 Myr, potentially associated with structural or phase transitions in Earth's interior. The model is compared with Earth's data derived from oceanic crust data, neglecting lateral extension of the continental crust. The observed behavior of Earth's data suggests the possibility of additional viscosity weakening toward the most recent epoch, or/and an increase of effective elasticity.

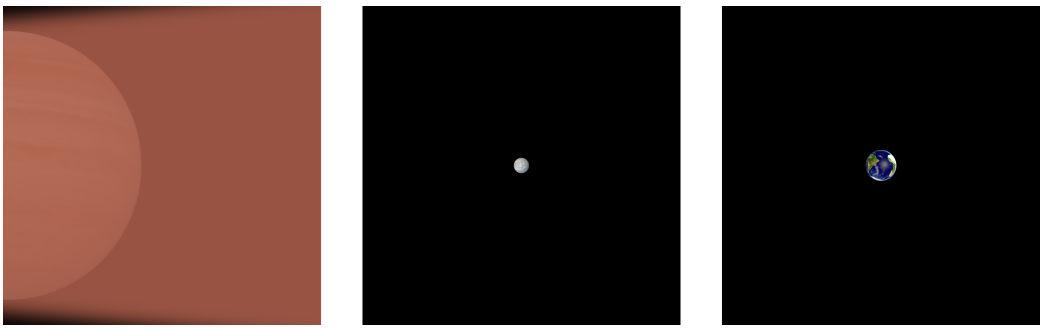

Figure 8: Artist's impressions of Earth at three evolutionary stages: (left) gas-giant stage at formation (≈ 4.56 Ga) with a photoevaporation envelope (the Sun is located to the left of the gas giant, and the colors of the planet and its elongated envelope have been enhanced for visibility); (center) first mechanical era of a metastable chthonian Earth, farther from the Sun, until ~ -200 Myr, possibly covered by an icy crust; (right) present-day Earth.

Table 3: First ionization energies [17], Earth abundances, atomic proportions, and contributions to the mean ionization energy for major terrestrial elements. Adapted from McDonough [22].

Element	First Ionization Energy [eV]	Earth (wt%)	Atomic Proportions	Fraction of Mean Ionization Energy [eV]
Fe	7.90	32.00	0.15	1.19
O	13.62	29.70	0.48	6.54
Si	8.15	16.10	0.15	1.22
Mg	7.65	15.40	0.17	1.30
Ni	7.64	1.82	0.01	0.08
Ca	6.11	1.71	0.01	0.06
Al	5.99	1.59	0.02	0.12
S	10.36	0.64	0.01	0.10
Cr	6.77	0.47	0.00	0.00
Na	5.14	0.18	0.00	0.00
P	10.49	0.07	0.00	0.00
Mn	7.43	0.08	0.00	0.00
C	11.26	0.07	0.00	0.00
H	13.60	0.03	0.01	0.14
Sum	-	99.86	1.00	10.74